Journal of Computers Vol. 29 No. 6, 2018, pp. 168-180
doi:10.3966/199115992018122906016

Wavelet-based Technique for Mobile Device with Low Resolution Depth Image-based Rendering

Shengrong Lu[1], Chih-Hsien Hsia[2,7*], Wei-Han Cheng[3], Hsin-Ting Li[3], Jen-Shiun Chiang[3], Ling Zhang[1], Hsien-Wei Tseng[1], Cihun-Siyong Alex Gong[4,5,6]

[1] School of Information Engineering, Longyan University, Longyan city 364012, Fujian, China

[2] Department of Computer Science and Information Engineering, National Ilan University, Yilan, Taiwan
chhsia625@gmail.com

[3] Department of Electrical and Computer Engineering, Tamkang University, New Taiepi, Taiwan

[4] Department of Electrical Engineering, Chang Gung University, Taoyuan, Taiwan

[5] Portable Energy System Group of Green Technology Research Center, Chang Gung University, Taoyuan, Taiwan

[6] Department of Ophthalmology, Chang Gung Memorial Hospital, Taoyuan, Taiwan

[7] Master Program of Arts and Technology, Chinese Culture University, Taiwan

Received 9 January 2018; Revised 18 March 2018; Accepted 18 March 2018

Abstract. Depth Image-Based Rendering (DIBR) is an approach to generate a 3-D image by the original 2-D color image with the corresponding 2-D depth map. Although DIBR is ~~a~~ quite convenient to convert 2D images to 3D ones, there is a disadvantage in DIBR system that it cannot reach real-time processing due to the computing time. Against this, this paper proposes a method which is based on discrete wavelet transform and adaptive edge-oriented smoothing process, to speed up the computing of the system. The proposed method still preserves the original texture and thus the proposed method not only preserves the vertical texture but also reduces at least 60% of the computing time of the DIBR system.

Keywords: asymmetric/symmetric smoothing filter, depth image-based rendering, discrete wavelet transform, image warping

1 Introduction

The three-dimensional (3-D) images have become more and more popular in our life. It provide~~s~~ users with a feeling of presence of 3-D view from simulation of reality. Generally, a stereoscopic image~~s~~ must be synthesized by at least two or more 2-D images and consequently it needs more than two times of both transmission time and storage space in the coding and transmission stage. European IST started the ATTEST project [1], in which they proposed a Depth Image-Based Rendering (DIBR) technology so that the image for 3-D synthesis can be generated from a single 2-D image and the corresponding depth map to improve the deficiency of the traditional 3-D TV. The DIBR technology not only reduces the transmission time but also reduces storage space of images. There are some factors that affect the quality of DIBR: (1) Occlusion and disocclusion generated by image warping; (2) Imperfect depth map; (3) It cannot preserve the completed horizontal and vertical textures. Occlusion will happen after image warping because the background pixels and foreground pixels may overlap. The foreground pixels can be used to replace the background pixels [2] to resolve the occlusion. Disocclusion usually takes place on the edge of the foreground and background of the depth map. It will appear in the newly exposed areas

* Corresponding Author

(called "holes") in the virtual image after warping. Several approaches were proposed to fill the holes, such as interpolation [3], extrapolation [3], mirroring [4], and image inpainting [4]. Chen et al. [5] proposed an approach by using a smoothing filter on the depth map to reduce the holes. However, this approach is not good to preserve the vertical texture. To solve this problem, Zhang et al. [7] used the asymmetric smoothing filters to preserve the vertical texture. However, using asymmetric smoothing filters to process the whole depth map may destroy the horizontal texture. Against this, Lee et al. [8] proposed a smoothing filter based on the analysis of vertical texture to overcome the difficulties. Tam et al. [6] used the symmetric smoothing filter to process the weaker vertical texture, and used the asymmetric smoothing filter [7] to process the stronger vertical texture, and through such an arrangement, the disocclusion artifacts were incrementally removed as the smoothing of depth maps became stronger. This approach can reduce the geometric distortions as well.

Although the above methods can preserve the vertical and horizontal textures of an image, computing takes a long time. Against this background, this study proposes a new wavelet-based rendering approach to lower the resolution. The proposed method utilizes the characteristic of DWT to save the high frequency domain information, and ~~it~~ uses both symmetric Gaussian filter and asymmetric Gaussian filter to strengthen the vertical texture after image warping. The experimental results indicate that the proposed method not only preserves vertical texture but also largely reduces the computation time.

The rest of this paper is organized as follows. In Section 2, the traditional DIBR system flow is introduced. Section 3 describes the proposed method in detail. Section 4 compares the proposed method with other related research works. Finally we conclude in Section 5.

2 Depth Image-Based Rendering

In the traditional DIBR system, first, the system reads the original depth map and uses the smoothing filter to preprocess the depth map for reducing holes generated after image warping. Then the system reads the original color image and processes the depth map to generate the virtual left view or the virtual right view by warping. Finally, the system tries to fill the holes which were generated in the virtual left view or the virtual right view after image warping. Fig. 1. shows the system flow.

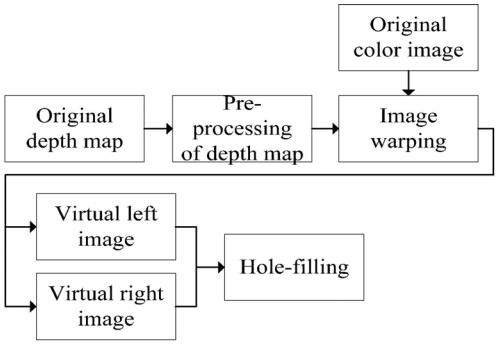

Fig. 1. Flowchart of the system of DIBR

2.1 Pre-Processing of Depth Map

Pre-processing of the depth map is to reduce the number of holes in the virtual left and virtual right views. Because the holes usually appeare on the edge of sharp depth discontinuities, it needs to use smoothing filters [6-7] to smooth the depth map. The smoothing filters can be classified into two categories: symmetric Gaussian filter [6] and asymmetric Gaussian filter [7]. Generally the Gaussian filters are expressed as (1):

$$g(x,\sigma_\mu)=\frac{1}{\sqrt{2\pi}\sigma_\mu}\exp\{-\frac{x^2}{\sigma_\mu^2}\}\ for-\frac{\omega}{2}\le x\le\frac{\omega}{2},$$
$$g(y,\sigma_v)=\frac{1}{\sqrt{2\pi}\sigma_v}\exp\{-\frac{x^2}{\sigma_v^2}\}\ for-\frac{\omega}{2}\le y\le\frac{\omega}{2}. \quad \textbf{(1)}$$

where $g(x,\sigma_\mu)$ represents the horizontal Gaussian function, $g(y,\sigma_v)$ the vertical Gaussian function,

σ_μ the horizontal direction deviation, σ_v the vertical direction deviation, x and y the locations of the horizontal and vertical axises, respectively, and ω the window size of the filter. The symmetric and asymmetric Gaussian filters are different from their deviations. For the symmetric Gaussian filter, deviations σ_μ and σ_v are the same, and the values of the window sizes of the filters, ω, are also the same in the vertical and horizontal directions. However, for the asymmetric Gaussian filters, deviations σ_μ and σ_v are different, and the values of the window sizes of the filters, ω, are also different from the vertical and horizontal directions.

Tam et al. [6] proposed a symmetric smoothing filter ($\sigma_\mu = \sigma_v$) to preprocess the whole depth map as shown in Fig. 2. From Fig. 2(b) we can find the virtual left image is smoothed by the symmetric smoothing filter after warping. After preprocessing by the symmetric smoothing filter, it can largely reduce the number of holes, but the information of the vertical texture is destroyed as shown in Fig. 2(c). We can find that the symmetric smoothing filter cannot preserve the vertical texture of the leg of the table such that the stronger vertical texture is distorted. Therefore, Zhang et al. [7] proposed an asymmetric smoothing filter ($\sigma_\mu < \sigma_v$) to solve the problem of decaying vertical texture. The asymmetric smoothing filter increases the ratio of σ_v to σ_μ and that of ω in the vertical direction to ω in the horizontal direction, and therefore the strength of the vertical texture can be enhanced. As shown in Fig. 3(a), the approach proposed by Zhang et al. uses the asymmetric smoothing filter to smooth the whole depth map. Obviously, the leg of the table in the depth map preserves a better vertical texture than that shown in Fig. 2(a). It means after image warping, the leg of the table as shown in Fig. 3(c) preserves more completely than that of Fig. 2(c). However, both symmetric smoothing filter and asymmetric smoothing filter may cause some distortion of the virtual image. It weakens the vertical texture or horizontal texture, because the smoothing filters smooth the whole depth map with the symmetric smoothing filter or asymmetric smoothing filter. Besides, the symmetric/asymmetric smoothing filter also increases the computing time; to overcome this difficulty we propose a method to decrease the computing time and further preserve the stronger texture information.

(a) the depth map preprocessed by a symmetric smoothing filter with $\sigma_\mu = \sigma_v = 30$

(b) the virtual left view

(c) the focus on the leg of the table

Fig. 2. Diagram showing toggling and swapping Symmetric Gaussian filter results

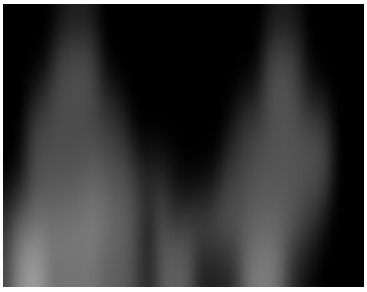

(a) the depth map preprocessed by a asymmetric smoothing filter with $\sigma_\mu = 10$ and $\sigma_v = 90$

(b) the virtual left view

(c) the focus on the leg of the table

Fig. 3. Asymmetric Gaussian filter results

2.2 Image Warping and Hole Filling

Image warping plays an important role in the DIBR system. It uses depth map to calculate the parallax value of every pixel and then uses the parallax value to calculate the distance of left shift or right shift to generate the virtual left view or virtual right view. Based on the shift-sensor approach [9], the virtual left view or virtual right view can be generated from the following (2):

$$X_l = X_c + \frac{t_x}{2}\frac{f}{Z}, X_r = X_c + \frac{t_x}{2}\frac{f}{Z}, \tag{2}$$

where X_l and X_r are the pixel coordinates of the virtual left view and virtual right view, respectively, X_c the pixel coordinate of the original color image, t_x the baseline distance between the left and right cameras, f the focal length, and Z the depth distance from the camera to the object.

After image warping, the virtual view will expose holes. Because the system has preprocessed the depth map, the number of holes can be largely decreased. Therefore, it only needs to use the mirroring method to fill the holes generated by the neighbor pixels.

3 Proposed Methodology

Fig. 4 shows the flowchart of the new DIBR system with our proposed method. This approach can preserve not only the horizontal and vertical textures but also the completed information of the non-hole region, and it can reduce the computing time significantly. The proposed method adopts the adaptive smoothing filter approach [8], which uses the symmetric smoothing filter [6] and asymmetric smoothing filter [7] to preserve the information of the horizontal and vertical textures and the completed depth map information of the non-hole region. To reduce the computation time, the Discrete Wavelet Transform (DWT) algorithm was also applied [10-12] in our DIBR system.

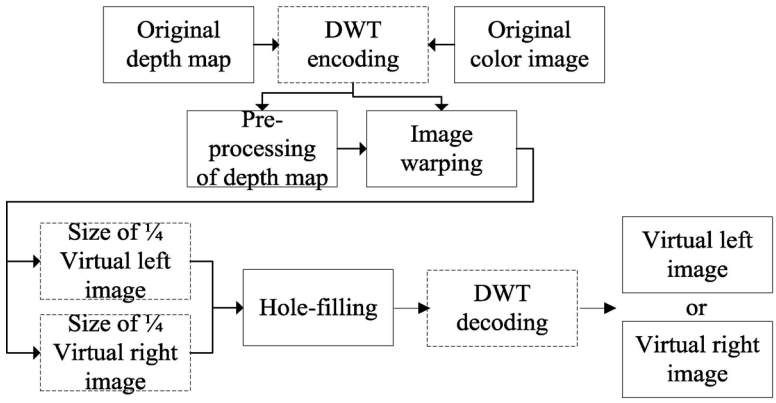

Fig. 4. Flowchart of the proposed DIBR system

3.1 Low Resolution Method

To decrease the computing time, this work adopts DWT to scale down the resolution of the color image and depth map. Conventionally, people use Down Sampling (DS) and Average Filter (AF) scheme to scale down the resolution of an image [13-16]. However, those DS schemes cannot efficiently preserve good information of the original image, in contrast, it easily causes distortion after recovering the image back to the original size. On the other hand, the AF scheme takes the neighbor pixels and itself to calculate the average value to scale down the resolution, so that the image is blurred after resolution scaling down. Therefore, both methods are not suitable for the DIBR system. In recent years, some researchers used DWT scheme [17-19] for resolution scaling due to the fantastic concentration characteristics and natural multiresolution character. It can also process each component separately. During the signal decomposition, it can reduce the sampling times to avoid repetition. When recovering signals, it must increase the up-sampling rate. The converted signal can also reduce the relativity of the input signal efficiently. In this research work we use a mask to complete the encoding and decoding of

DWT [12]. The mask coefficients for HH-band, LH-band, LL-band, and HL-band are respectively shown in equations (3)-(6):

$$HH(i,j) = x(2i+2j+1) + \frac{1}{4}\sum_{u=0}^{1}\sum_{v=0}^{1} x(2i+2u, 2j+2v) + (-\frac{1}{2})\sum_{u=1}^{2} x(2i+|u|, 2j+|1-u|). \quad \textbf{(3)}$$

$$\begin{aligned} LH(i,j) = {} & \frac{3}{4}x(2i, 2j+1) + \frac{1}{16}\sum_{u=0}^{1}\sum_{v=0}^{1} x(2i-2+2u, 2j+4v) + (-\frac{1}{8})\sum_{u=0}^{1} x(2i, 2j+4u) \\ & + \sum_{u=0}^{1}\sum_{v=0}^{1} x(2i-1+2u, 2j+2v) + (\frac{1}{4})\sum_{u=0}^{1} x(2i-1+2u, 2j+1) + (-\frac{3}{8})\sum_{u=0}^{1} x(2i, 2j+2u). \end{aligned} \quad \textbf{(4)}$$

$$\begin{aligned} LL(i,j) = {} & (\frac{9}{16})x(2i, 2j) + \frac{1}{64}\sum_{u=0}^{1}\sum_{v=0}^{1} x(2i-2+4u, 2j+4v) + \frac{1}{16}\sum_{u=0}^{1}\sum_{v=0}^{1} x(2i-1+2u, 2j-1+2v) \\ & + (-\frac{1}{32})\sum_{u=0}^{1}\sum_{v=0}^{1} x(2i-1+2u, 2j-2+4v) + (-\frac{1}{32})\sum_{u=0}^{1}\sum_{v=0}^{1} x(2i-2+4u, 2j-1+2v) \\ & + (\frac{3}{16})\sum_{u=0}^{1}[x(2i-1+2u, 2j) + P(2i, 2j-1+2u)] + (-\frac{3}{32})\sum_{u=0}^{1}[x(2i-2+4u, 2j) + x(2i, 2j-2+4u)]. \end{aligned} \quad \textbf{(5)}$$

$$\begin{aligned} HL(i,j) = {} & \frac{3}{4}x(2i+1, 2j) + \frac{1}{16}\sum_{u=0}^{1}\sum_{v=0}^{1} x(2i+4u, 2j-2+2v) + (-\frac{1}{8})\sum_{u=0}^{1} x(2i+4u, 2j) \\ & + (-\frac{1}{8})\sum_{u=0}^{1}\sum_{v=0}^{1} x(2i+2u, 2j-1+2v) + (\frac{1}{4})\sum_{u=0}^{1} x(2i+1, 2j-1+2u) + (-\frac{3}{8})\sum_{u=0}^{1} x(2i+2u, 2j). \end{aligned} \quad \textbf{(6)}$$

where (i,j) is the location of the coefficients. Because of using the LL-band of DWT to get the complete object information, the results of preprocessing in depth map, image warping, and hole filling in the color image are very stable. The DWT of an image separates the whole image into four sub-bands: HH-band, HL-band, LH-band, and LL-band. However, only the LL-band preserves most of the information of the original image. Therefore, only the LL-band of the DWT is used in the operation of image rendering and other sub-bands are retained for the IDWT operation.

3.2 Adaptive Smoothing Filter

In Fig. 5, to preserve the completeness of the depth map, this paper uses the following equation to predict the holes to avoid the distortion after the smoothing process in the non-hole region:

$$Label(x,y) = \begin{cases} 1, \text{ if } s(x+1,y) - s(x,y) > Th_0 \\ \quad \text{for the left view} \\ \text{if } s(x-1,y) - s(x,y) > Th_0 \\ \quad \text{for the right view} \\ 0, \text{ otherwise} \end{cases} \quad \textbf{(7)}$$

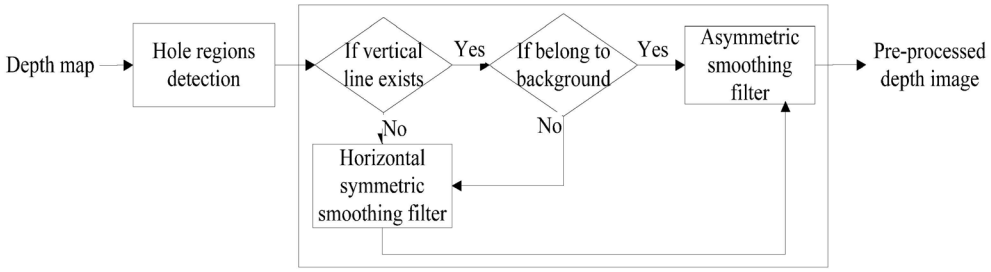

Fig. 5. The flowchart of the adaptive smoothing filter

where the threshold value Th_0 is set to 20 and $s(x,y)$ represents the value of depth at (x,y). The following equation can be used to find out the information with vertical texture in the depth map.

$$V_{\in}(x, y+q)=\begin{cases}1, \text{if } |p_q * G| > Th_1 \\ \quad \text{where } s(x, y+q) < s(x, y) + Th_0 \\ \quad \text{and } Label(x, y) = 1 \\ 0, \text{otherwise}\end{cases} \tag{8}$$

where $q \in \{1,2,...,r\}$, or $q \in \{-1,-2,...,-r\}$; $p_q = \hat{p}(x, y+q)$; operator "*" means convolution; and is a 3×3 vertical Sobel mask to find the vertical texture feature. We can use (8) together with the information found from (7) to label the hole pixels with the vertical texture. Equation (10) can be used to find out the vertical line:

$$G=\begin{bmatrix}1 & 0 & -1 \\ 2 & 0 & -2 \\ 1 & 0 & -1\end{bmatrix} \tag{9}$$

$$V_L(x, y)=\begin{cases}1, \text{if } \dfrac{\sum_{q=1}^{r} V_{\in}(x, y+q)}{r} \geq Th_2 \\ \quad \text{or } \dfrac{\sum_{q=-1}^{-r} V_{\in}(x, y+q)}{r} \geq Th_2 \\ 0, \text{otherwise}\end{cases} \tag{10}$$

where $V_L(x, y) = 1$ represents the detected vertical line information. We can use (8) and (10) to find a stronger vertical texture.

This paper uses the asymmetric smoothing filter [7] at the pixels labeled by (10) with vertical line ($V_L(x, y) = 1$, $Label(x, y) = 1$) and uses the symmetric smoothing filter at other hole pixels ($Label(x, y) = 1, V_L(x, y) \neq 1$).

3.3 Enhancement of the Vertical Texture Using Adaptive Smoothing Filter

To enhance the vertical texture of the depth map, we label the pixels on the depth map of the virtual left view as the pixels of the vertical lines and the N pixels resided in the right side of the pixel are labeled as 1. Besides, we label the upper and lower i pixels of the current pixel as 1 ($V_L(x+M, y)=1$, $M \in \{1,2,...,N\}$). The pixels in the right virtual view are labeled toward left. The horizontal holes do not need to be changed. Finally we combine the DWT technique and adaptive smoothing filter scheme to accomplish our DIBR operation. In our approach the color image and the depth map are encoded by DWT first then the adaptive smoothing filter is used to process the LL-band of the depth map. Besides the situations when the processed color image and depth map are used in the image warping and the color image is used in hole filling, the LL-band is not needed in the DWT decoding, and therefore it can reduce the computation time significantly. After the adaptive smoothing filter processing, DWT decoding will be applied to recover the image back to its original size. Fig. 4 shows the DIBR operation flow. Fig. 6(a) to Fig. 6(c) show the original depth map, and Fig. 6(d) to Fig. 6(f) are the processed depth maps after DWT by using the adaptive smoothing filter scheme in the LL-band. It can be found that the LL-band of the depth map still preserves the completed depth information in the non-hole region.

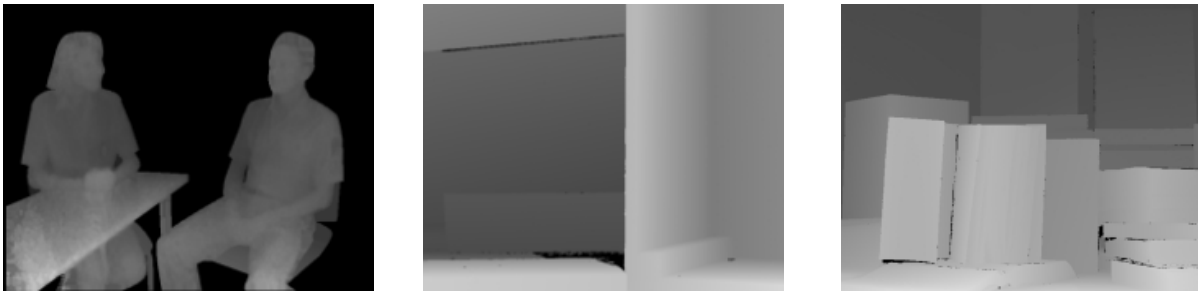

(a) the original depth maps (b) the original depth maps (c) the original depth maps

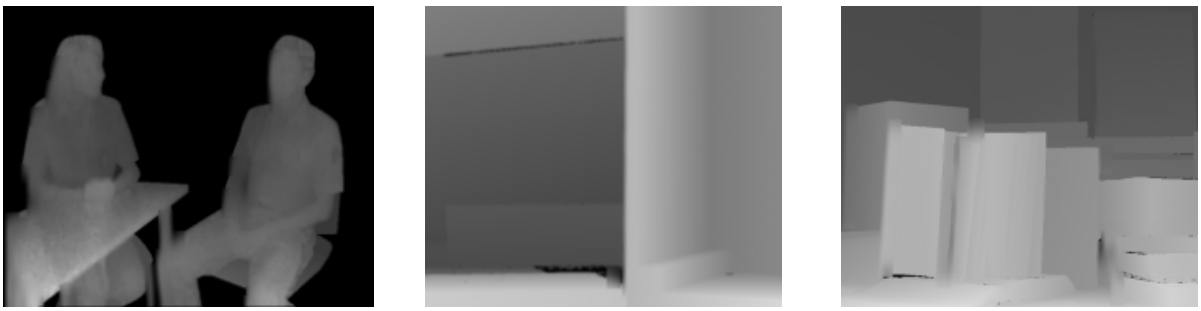

(d) the processed depth maps by using LL-band ($N = 20$, $i = 20$) (e) the processed depth maps by using LL-band ($N = 20$, $i = 20$) (f) the processed depth maps by using LL-band ($N = 20$, $i = 20$)

Fig. 6. Depth maps

4 Experimental Results and Comparison

Compared with the previous research works, the proposed DIBR system can reduce the computing complexity and preserve the information of the horizontal and vertical textures. Here we use one order DWT to process the images and depth maps. And the reason to do this is that more orders may result in a worse quality after the system recovering the image back to the original size because the phase shifting of the LL-band and the phases of other sub-bands remain unchanged. The higher order of DWT may cause more phase shifting and thus it will lead to worse qualities. This symptom is depicted in Fig. 7(b). In Fig. 7, we can find that the quality shown in Fig. 7(b) is worse than that in Fig. 7(a), and this may cause an uncomfortable experience in viewing the video sequence.

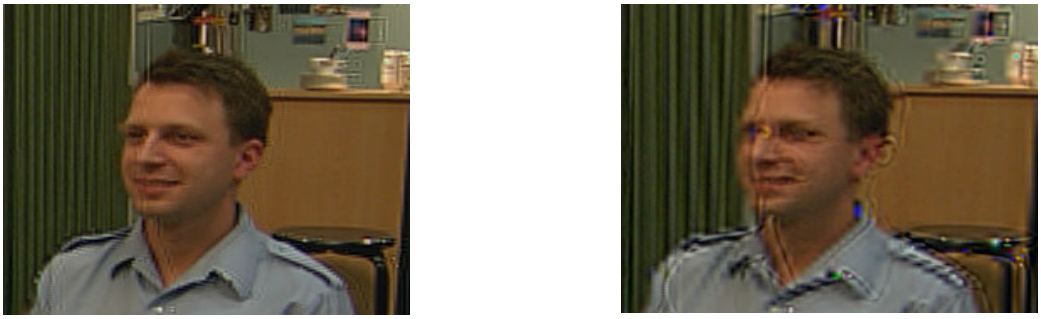

(a) the image processed by the first order DWT after using the proposed method (b) the image processed by the second order DWT after using the proposed method

Fig. 7. DWT order comparisons

4.1 Testing Image and Parameter Selection

Fig. 8 shows three images selected from the Middlebury data set [20]. These three images include Interview, Wood, and Books, and their sizes are 720 × 576, 686 × 555, and 695 × 555, respectively.

(a) are "Interview" and its corresponding depth map, respectively

(b) are "Wood" and its corresponding depth map, respectively

(c) are "Books" and its corresponding depth map, respectively

(d) are "Interview" and its corresponding depth map, respectively

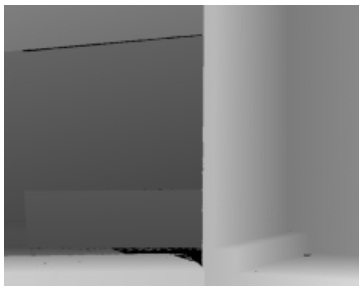

(e) are "Wood" and its corresponding depth map, respectively

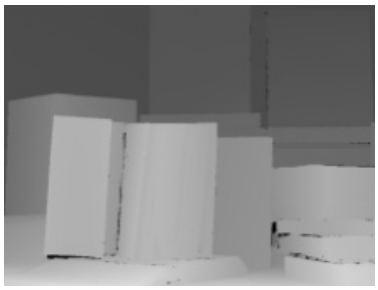

(f) are "Books" and its corresponding depth map, respectively

Fig. 8. Test image

To make people watch a 3-D TV comfortably, the depth distance range of the virtual view must be selected in advance. According to the document records, the most comfortable distance to watching TV is about 5% of a standard picture (43 height). With a focal (*f*) of 1. However, after calculating, the baseline distances for "Interview", "Wood", and "Books" are 36, 34, and 35, respectively. From [19], the selected baseline distance in this research is set to 20 which is smaller than the largest value. The chosen strength of the horizontal depth smooth) is set to one-quarter of the baseline distance. When the smoothing strength reaches some limited value, the quantities of holes become constant [7]. Therefore we do not need to increase the smoothing strength unlimitedly, which may increase the computing time. For symmetric Gaussian filters, the horizontal and vertical smoothing strengths are equal ($\sigma_\mu = \sigma_v$). For asymmetric Gaussian filters, theoretically the vertical smoothing strength (σ_v) is 5 times stronger than the horizontal smoothing strength (σ_μ) ($\sigma_v = 5\sigma_\mu$). In this experiment, the sizes of the symmetric and asymmetric filters are 3 times of the depth smoothing strength (σ). Other thresholds are selected as 4 and 6, i.e. $Th_1 = 50$, $Th_2 = 0.5$, and $r = 20$. Because the DWT operation shrinks the image to one-quarter of the original size, we count the size of baseline distance as that after scaling down. Table 1 shows the related deviation values of both references [6-8] and our work.

Table 1. Standard deviation configuration

Methods	σ_μ	σ_v
Tam et al. [6]	30	30
Zhang et al. [7]	10	90
Lee and Effendi [8]	5	90
This Work	2	60

4.2 Results and Comparisons

Fig. 9 demonstrates the results processed by the method proposed in [6]. The vertical texture is completely destroyed. Fig. 10 indicates that the method proposed in [7] solves the vertical texture destroyed problems. Since this approach modifies the whole image even the places without holes, it cannot keep the completeness of the depth maps and also increase the computation times. Fig. 11 and Fig. 12. show the experimental results proposed in both [8] and our work. As what we can see, both results retain good horizontal and vertical textures, and neither our approach nor that of [8] alters the depth maps when there are no holes. However, the computation time of our approach is much less than that of [8].

(a) the generated virtual left view

(b) the corresponding depth map after preprocessing

Fig. 9. Use symmetric smoothing filter only

(a) the generated virtual left view

(b) the corresponding depth map after preprocessing

Fig. 10. Use asymmetric smoothing filter only

(a) the generated virtual left view

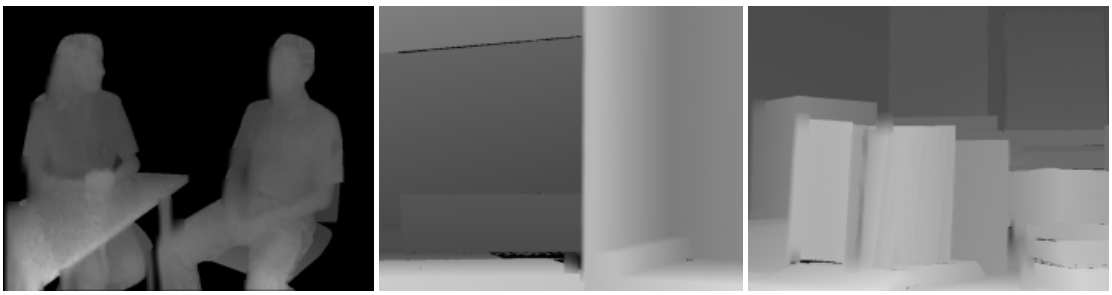

(b) the corresponding depth map after preprocessing

Fig. 11. Use adaptive smoothing filters

(a) the generated virtual left view

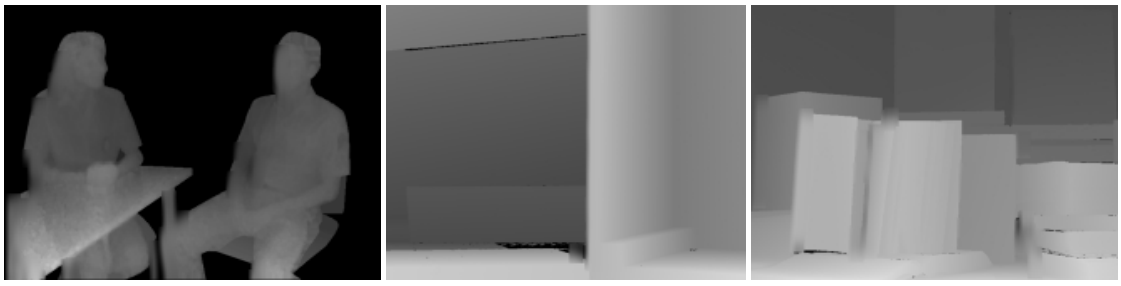

(b) the corresponding depth map in the LL-band after preprocessing

Fig. 12. Use the proposed method

Fig. 13 shows the enlarged images of the vertical textures that were operated by the methods proposed in [7-8], and ours, respectively; the results are almost the same. Table 2 addresses the PSNR and operation times for various approaches. Regarding to performance and quality, our proposed approach is outperformed.

(a) The enlargement of the leg of the table after the asymmetric smoothing filter processing

(b) The enlargement of the leg of the table after the adaptive smoothing filter processing

(c) The enlargement of the leg of the table after proposed method processing

Fig. 13. Image quality

Table 2. PSNR and computation time comparison

Image	Methods	PSNR(dB)	Time(ms)
Interview	Tam et al. [6]	18.41	25237
	Zhang et al. [7]	18.41	10939
	Lee and Effendi [8]	18.46	1143
	This Work	18.48	413
Wood	Tam et al. [6]	23.86	21889
	Zhang et al. [7]	24.57	9473
	Lee and Effendi [8]	24.57	655
	This Work	24.35	270
Books	Tam et al. [6]	18.51	22266
	Zhang et al. [7]	18.60	9330
	Lee and Effendi [8]	18.60	1368
	This Work	18.43	311

5 Conclusion

In this paper, the low resolution technique and adaptive smoothing filter schemes are applied for DIBR. The low resolution with DWT technique can reduce the computation time significantly. The adaptive smoothing filter can retain the horizontal and vertical textures very well. The experimental results show that our proposed method not only retains the texture of the original image but reduces 60% of system computing time. This work analyzed an efficient DIBR system for the algorithms of the depth imaging compensation method. It approach can also handle multi-view schemes and provide good 3D view qualities.

Acknowledgements

The authors would like to thank the anonymous reviewers of their paper for the many helpful suggestions. This work was supported by the Ministry of Science and Technology of Taiwan, under grant number MOST-103-2221-E-034-010-. Then, this work was supported by the Education Scientific Research Project of Young Teachers of Fujian Province under grant number JAT170577, the climbing project of Longyan University under grant number LQ2015031, Fujian university's key lab. of bigdata mining and application and Collaborative innovation project of Longyan University(L. Zhang). Final this work was supported by the Chang Gung Memorial Hospital of Taiwan, under grant number CMRPD2F0102.

References

[1] A. Redert, M.O. de Beeck, C. Fehn, W. Ijsselsteijn, M. Pollefeys, L.V. Gool, E. Ofek, I. Sexton, P. Surman, ATTEST:

advanced three-dimensional television system technologies, in: Proc. 2002 International Symposium on 3D Data Processing Visualization and Transmission, 2002.

[2] Q.H. Nguyen, M.N. Do, S.J. Patel, Depth image-based rendering from multiple cameras with 3D propagation algorithm, in: Proc. 2009 International Conference on Immersive Telecommunications, 2009.

[3] C. Vázquez, W.J. Tam, F. Speranza, Stereoscopic imaging: filling disoccluded areas in depth image-based rendering, in Proc. Society of Photo-Optical Instrumentation Engineers (SPIE) Conference Series, 2006.

[4] C.-M. Cheng, S.-J. Lin, S.-H. Lai, J.-C. Yang, Improved novel view synthesis from depth image with large baseline, in: Proc. 2008 International Conference on Pattern Recognition, 2008.

[5] W.-Y. Chen, Y.-L. Chang, S.-F. Lin, L.-F. Ding, L.-G. Chen, Efficient depth image based rendering with edge dependent depth filter and interpolation, in: Proc. 2005 IEEE International conference on Multimedia and Expo, 2005.

[6] W. J. Tam, G. Alain, L. Zhang, T. Martin, R. Renaud, Smoothing depth maps for improved stereoscopic image quality, in Proc. Society of Photo-Optical Instrumentation Engineers (SPIE) Conference Series, 2004

[7] L. Zhang, W. J. Tam, Stereoscopic image generation based on depth images for 3DTV, IEEE Transactions on Broadcasting 51(2)(2005) 191-199.

[8] P.-J. Lee, Effendi, Nongeometric distortion smoothing approach for depth map preprocessing, IEEE Transactions on Multimedia 13(2)(2011) 246-254.

[9] A. Woods, T. Docherty, R. Koch, Image distortions in stereoscopic video systems, in: Proc. Society of Photo-Optical Instrumentation Engineers (SPIE) Conference Series, 1993.

[10] T. Vijayaraghavan, K. Rajan, Image coding of 3D volume using wavelet transform for fast retrieval of 2D images, Proceedings of IEE on Image and Signal Processing, Vision 153(4)(2006) 507-511.

[11] M. Ravasi, L. Tenze, M, Mattavelli, A scalable and programmable architecture for 2-D DWT decoding, IEEE Transactions on Circuits and Systems for Video Technology 12(8)(2002) 671-677.

[12] C.-H. Hsia, J.-M. Guo, J.-S. Chiang, Improved low-complexity algorithm for 2-D integer lifting-based discrete wavelet transform using symmetric mask-based scheme, IEEE Transactions on Circuits and Systems for Video Technology 19(8)(2009) 1202-1208.

[13] B. Sugandi, H. Kim, J.K. Tan, S. Ishikawa, Real time tracking and identification of moving persons by using a camera in outdoor environment, International Journal on Innovative Computing, Information and Control 5(5)(2009) 1179-1188.

[14] J.-C. Huang, W.-S. Hsieh, Wavelet-based moving object segmentation, Electronics Letters 39(39)(2003) 1380-1382.

[15] S. Cvetkovic, P. Bakker, J. Schirris, P.H.N. de With, Background estimation and adaptation model with light-change removal for heavily down-sampled video surveillance signals, in: Proc. 2006 IEEE International Conference on Image Processing, 2006.

[16] Y.-L. Tian, A. Hampapur, Robust salient motion detection with complex background for real-time video surveillance, in: Proc. 2005 IEEE Workshop on Motion and Video Computing, 2005.

[17] F.-H. Cheng, Y.-L. Chen, Real time multiple objects tracking and identification based on discrete wavelet transform, Pattern Recognition 39(3)(2006) 1126-1139.

[18] C.-H. Hsia, J.-M. Guo, Improved directional lifting-based discrete wavelet transform for low resolution moving object detection, in: Proc. 2012 IEEE International Conference on Image Processing, 2012.

[19] C.-H. Hsia, W.-H. Cheng, H.-T. Li, J.-S. Chiang, Spatial domain complexity reduction method for depth image based rendering using wavelet transform, in: Proc. 2013 IEEE International Symposium on Intelligent Signal Processing and Communications Systems, 2013.

[20] Middlebury stereo vision. <http://vision.middlebury.edu/stereo/data/>, 2002 (accessed 18.03.18).